



## Embedding Aromatic Conjugated Monomer within Carbon Nitride for Efficient Photocatalytic Reduction Reactions



Zeeshan Ajmal<sup>a</sup>, T.A. Taha<sup>b,c</sup>, Mohammed A. Amin<sup>d</sup>, Arkom Palamanit<sup>e</sup>, W.I. Nawawi<sup>f</sup>, Abul Kalam<sup>g,h</sup>, Abdullah G. Al-Sehemi<sup>g,h</sup>, Hamed Algarni<sup>g,i</sup>, Abdul Qadeer<sup>j</sup>, Hamid Ali<sup>k</sup>, Anuj Kumar<sup>l</sup>, Jin Qian<sup>a,\*</sup>, Asif Hayat<sup>m,n,\*</sup>, Huaqiang Zeng<sup>a,\*</sup>

<sup>a</sup> School of Chemistry and Chemical Engineering, Northwestern Polytechnical University, Xian, China

<sup>b</sup> Physics Department, College of Science and Arts, Jouf University, P.O. Box 756, Al-Gurayat, Saudi Arabia

<sup>c</sup> Physics and Engineering Mathematics Department, Faculty of Electronic Engineering, Menoufia University, Menouf 32952, Egypt

<sup>d</sup> Department of Chemistry, College of Science, Taif University, P.O. Box 11099, Taif 21944, Saudi Arabia

<sup>e</sup> Energy Technology Program, Department of Specialized Engineering, Faculty of Engineering, Prince of Songkla University, 15 Karnjanavanich Rd., Hat Yai, Songkhla 90110, Thailand

<sup>f</sup> Faculty of Applied Sciences, Universiti Teknologi MARA, Cawangan Perlis, 02600 Arau, Perlis, Malaysia

<sup>g</sup> Research Center for Advanced Materials Science (RCAMS), King Khalid University, P.O. Box 9004, Abha 61413, Saudi Arabia

<sup>h</sup> Department of Chemistry, College of Science, King Khalid University, P.O. Box 9004, Abha 61413, Saudi Arabia

<sup>i</sup> Department of Physics, Faculty of Science, King Khalid University, P.O. Box 9004, Abha 61413, Saudi Arabia

<sup>j</sup> State Key Laboratory of Environmental Criteria and Risk Assessment, National Engineering Laboratory for Lake Pollution Control and Ecological Restoration, Chinese Research Academy of Environmental Sciences, 10012 Beijing, China

<sup>k</sup> Multiscale Computational Materials Facility, Key Laboratory of Eco-Materials Advanced Technology, College of Materials Science and Engineering, Fuzhou University, Fuzhou 350100, China

<sup>l</sup> Nanotechnology Laboratory, Department of Chemistry, GLA, University, Mathura, Uttar Pradesh 281406, India

<sup>m</sup> College of Chemistry and Life Sciences, Zhejiang Normal University, Jinhua 321004, Zhejiang, China

<sup>n</sup> College of Geography and Environmental Sciences, Zhejiang Normal University, Jinhua 321004, China

### ARTICLE INFO

#### Article history:

Received 11 April 2022

Revised 5 October 2022

Accepted 13 October 2022

Available online 18 October 2022

#### Keywords:

Carbon nitride

Dibromobenzimidazole

Carbon dioxide reduction

Hydrogen evolution

Molecular engineering

### ABSTRACT

Due to a growing number of significant vitality and environmental issues, the standardized variation of carbon nitride (CN) for visible-light photocatalytic water splitting is an encouraging scientific topic. By revealing this, the functionalized monomer 2,6-dibromobenzimidazole (BI) was successfully embedded within the heptazine units of CN via a molecular engineering (Co-polymerization process) approach, and the as-synthesized product was named CN/BI<sub>x</sub>. Thereafter, as-synthesized materials were employed in the photocatalytic production of hydrogen (H<sub>2</sub>) via water splitting and CO<sub>2</sub> reduction into CO under visible light irradiance ( $\lambda = 420$  nm). Surprisingly, the substituent framework of CN, which was intimidated by the description of BI monomer, acted as a substitution reaction material and lubricated the electronic structure of CN by endorsing charge transition dissociation, which in turn boosted its photocatalytic performance under visible irradiation. The CN/BI<sub>10.0</sub> yields 62.8 mol of CO and 18.1 mol of H<sub>2</sub> for 4 h of the catalyzed reaction upon photooxidation under light irradiation, emphasizing the maximum photocatalytic performance with response to CO<sub>2</sub>. Correspondingly, the H<sub>2</sub> evolution rate (HER) for bulk CN was estimated as 17.6 mol/h<sup>1</sup>, whereas it was approximated as 203.7 mol/h<sup>1</sup> for CN/BI<sub>10.0</sub>, which is 10 times higher than that of CN. Such a phenomenon also predicts a substantial encroachment in the surface area, energy gap, and chemical properties, along with promotes the effective segregation of photoinduced charge separation from the valence band (VB) to the conduction band (CB) of CN, thereby, making it a good alternative for the photocatalytic water and CO<sub>2</sub> reduction reaction process.

© 2022 Elsevier B.V. All rights reserved.

\* Corresponding authors at: College of Chemistry and Life Sciences, Zhejiang Normal University, Jinhua 321004, Zhejiang, China (A. Hayat).

E-mail addresses: [qianjin@nwpu.edu.cn](mailto:qianjin@nwpu.edu.cn) (J. Qian), [asifncp11@yahoo.com](mailto:asifncp11@yahoo.com) (A. Hayat), [hqzeng@nwpu.edu.cn](mailto:hqzeng@nwpu.edu.cn) (H. Zeng).

### 1. Introduction

In the current era, the intensive use of carbon fuels and the accelerated release of carbon dioxide (CO<sub>2</sub>) into the worldwide ecosystem plays a significant role in human beings, by reducing fuel asset utilization levels, and thus, the constant ignition of these

fuels has been recognized as a convoluted task to humanity [1-7]. Even so, consistent efforts have been made to enhance the substantial alternatives for the subsequent transition of such carbon fuels into feasible chemical energy retrieval to investigate a green power source [8,9], in order to surmount such global pollution, and the economic downturn [10-14]. Researchers have focused their efforts on searching a good potential renewable source, that could be regarded as an unending clean sustainable energy source. Renewable irradiance, which is based on visible intensity, has distinctive techniques for reusing carbon fuels into beneficial chemical fuels in order to address environmental concerns and energy scarcity [15-22]. Even though, to proceed with such photo-fixation interactions, this transformation of fossil energy into feasible fuel assets requires a specialized form of broadening sunlight transformation feedstocks with considerable endeavor [23-27]. Semiconductor photocatalysts were used to replenish such zones, that are powered by illumination and have excellent photocatalytic performance for converting fossil fuels into electrical and chemical fuels [28-31]. This semiconducting photocatalyst mimics natural photosynthesis by absorbing illumination and inducing photocatalytic water splitting and CO<sub>2</sub> reduction reactions, captivating the production of hydrogen (H<sub>2</sub>), carbon monoxide (CO), methanol (MeOH), and methane (CH<sub>4</sub>) through photocatalysis [32-35]. Many systematic and innovation efforts have been stymied in their attempts to increase the photocatalytic efficiency of such semiconductors for the conversion of CO<sub>2</sub> into economically viable renewable inputs, as well H<sub>2</sub> energy, respectively [36-38]. A significant number of semiconductor materials are inappropriate for photoreduction of CO<sub>2</sub> source and water splitting processes, until massive renewable power owing to low consistency, high band gap, high cost or inactivity under visible region [39-41]. It is therefore, plausible to establish an efficient and appropriate photocatalyst with elevated consistency, low cost, metal free, and high activity for photocatalytic performance. Carbon nitride (CN) is metal-free photocatalyst of great interest, that is based on carbon (C) and nitrogen (N) which have a narrow band gap of 2.7 eV, and are inexpensive [42], thus, has increased accessibility and activity under visible light, and has excessive durability [43-47]. Such polymeric CN could be easily synthesized by the condensation of nitrogen-based precursors, that are inexpensive and accessible in essence and have better photocatalytic efficiency [48-55]. Regrettably, CN utilizes a modest portion of visible illumination due to a high proportion of charge replication, that reduced photoinduced electron carrier, and a minimal quantum yield, all of which contribute to reduced photocatalytic performance [56-59]. For this purpose, molecular engineering (copolymerization process) is a predefined approach, wherein we configure the aggregation of CN by hybridizing with well organic aromatic monomers in its framework in order to improve its optical absorption circumstances and  $\pi$ -dislocation system [60]. Correspondingly, such conjugated functionalized monomers integrate into the structure of CN to alter its electronic consistency, framework, and interfacial dynamics, as well as indicate a diverse intersection to speed up the charge mobility system, thereby endorsing CN photocatalytic performance [61,62].

In this paper, we orchestrated the procedure of molecular engineering by incorporating the distinctive organic aromatic monomer dibromobenzimidazole (BI) into the configuration of CN in order to improve its light absorptivity, by boosting the charge isolation, stimulate the electrons/holes conjugation, and empower the structural integrity, along with optical, and texture attributes of CN. Such alternation demonstrates a remarkable photocatalytic performance of CN for photocatalytic water reduction (H<sub>2</sub>) and CO<sub>2</sub> reduction (CO & H<sub>2</sub>) under visible light ( $\lambda = 420$  nm). The CN was simply obtained by the calcination of urea-based precursor as a starting material. The integrated BI

monomer composed of dibromo group that are replaced during molecular engineering and form a long polymer with large surface area, that produce more electrons for superior photocatalytic performance (Fig. 1). More importantly, the modulation of BI within CN alters a nucleophilic reaction between the amino group of BI and the triazine unit of CN. As a result of our prime alternative of this monomer, it anticipates a substantial divergence in the particular region, band gap, chemical properties, and configuration, as well as enhance the effective isolation of photoinduced charge transfer, thereby, making it a top contender for CO<sub>2</sub> reduction and water reduction into H<sub>2</sub> inputs.

## 2. Results and discussion

The X-ray diffraction (XRD) of materials reveals two distinct crystalline phase, as seen in Fig. 2a [63,64]. The predominant peak at 27.6° demonstrates the surface layer assembling of 2D covalently aromatic groups, whereas the modest peak at 12.6° is due to the in-plane compositional patterns of tri-s-triazine units. The Fourier transform infrared spectroscopy (FTIR) spectra illustrate that many peaks positioned at 1225-1580, 2950-3625, and 795 cm<sup>-1</sup> are associated to the traditional deformation, entrapped O-H compound, and breathing patterns of the s-triazine heterocyclic ring (C<sub>6</sub>N<sub>7</sub>) (Fig. 2b). According to XRD and FTIR, no visible granular variations in the fundamental crystalline phase or structure consistency of the CN component happen after molecular engineering.

The Brunauer-Emmett-Teller (BET) surface area of CN is 39.61 m<sup>2</sup>/g, and after the amalgamation of BI within the structure of CN, brought about the significant increase in the surface area of 168.49 m<sup>2</sup>/g for CN/BI<sub>10.0</sub> (Fig. 3a). Similarly, Fig. 3b depicts the pore-size distributions of Barrett-Joyner-Halenda (BJH) slope, which enhances as the quantity of BI increase within CN framework. Because surplus BI would not initiate a nucleophilic interaction via the amino group of urea, as it will disintegrate and discharge many gases during molecular engineering of CN. The surface area of all prepared materials is depicted in Table. S1.

Additionally, the photoluminescence transmittance [65] (PL) shifts from 461 nm to 483 nm toward a higher wavelength, thereby, lowering the band gap simultaneously (Fig. 4a). The PL spectra display that electrons/hole's agglomeration was accomplished in the CN framework in order to form the interfacial inter-actational heterojunctions due to robust charge linkage incorporated through molecular engineering. The diffuse reflectance (DRS) spectra represent a reduction in energy band gap due to the connection of introduced species within triazine architectural frame, thereby, resulting in to the efficient deformations in the HOMO and LUMO transition (Fig. 4b). The outcomes in turn show that copolymerized CN materials have significant visible-light adsorption performance as well as improved capabilities to capture light due to a constriction of the bandgap energy. The Table. S1 displays the band gap of all fabricated materials based on DRS calculations.

SEM images of CN and CN/BI<sub>10.0</sub> demonstrate nanoplatelets with spongy congested layers (Fig. 5a-b). The TEM appearance is fabric blended dendrimer bases for CN and copolymerized catalyst (Fig. 5c-d). The elemental mapping for superior sample CN/BI<sub>10.0</sub> is illustrated in Fig. 5e-h respectively.

X-ray photoelectron (XPS) analysis reveals the presence of carbon (C), nitrogen (N), and oxygen (O) in both catalysts, as proposed by wide XPS spectrum (Fig. S1). Two significant peaks were archived at 287.1, 284.5 eV (CN) and 288.4, 284.4 eV (CN/BI<sub>10.0</sub>), correlating to sp<sup>2</sup> hybridized carbon (N-C = N) and C-C single bonds on the surface of the material (Fig. 6a-b). Furthermore, the N 1s ranges for CN (398.3, 400.6, and 403.5 eV) and CN/BI<sub>10.0</sub> (398.9, 401.6, and 404.7 eV) represent the sp<sup>2</sup> hybridized N in the hep-

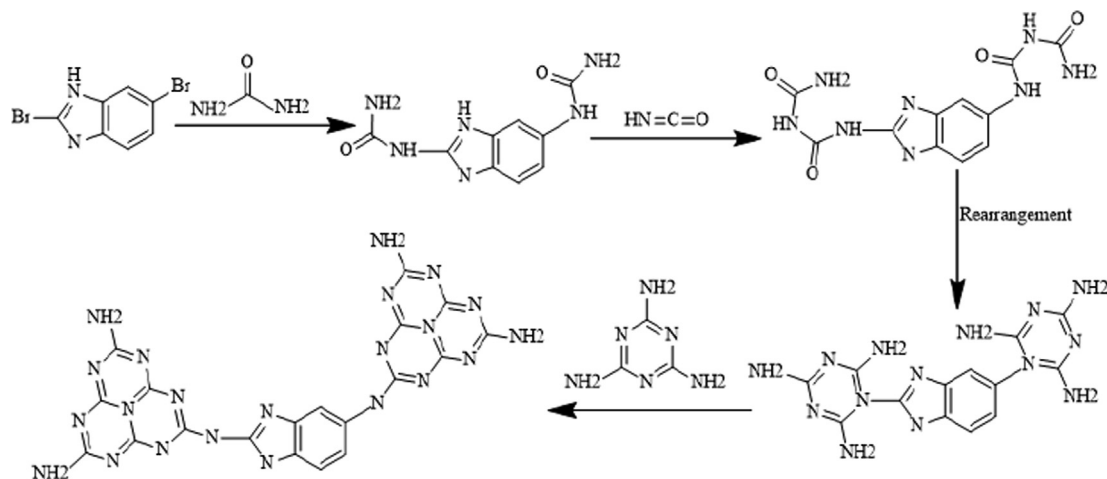


Fig. 1. Molecular engineering reaction process between CN and BI monomer.

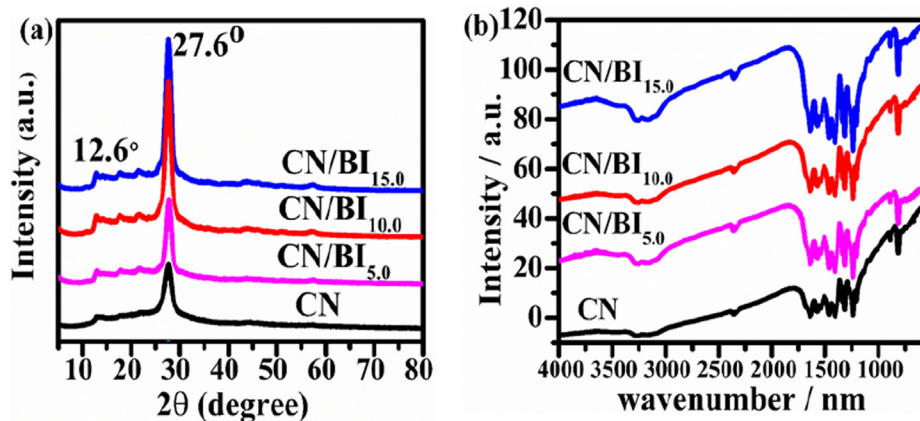


Fig. 2. (a) The XRD spectrum, and (b) FTIR spectroscopy of CN and BI-doped CN materials.

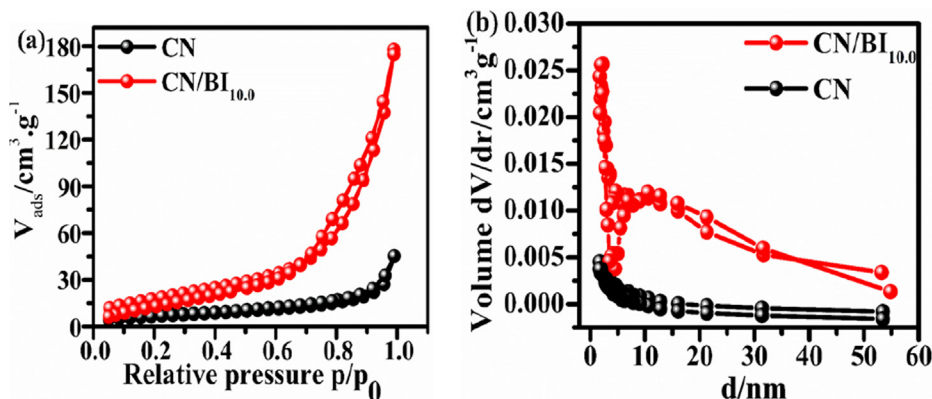


Fig. 3. (a) The  $N_2$ -sorption isotherm models for CN and CN-BI<sub>10.0</sub> catalysts, and (b) the associated BJH pore-size distribution patterns.

tazine ring (C-N=C), the amino configuration cluster (C-N-H), and the segmentation of the charging impact in the heptazine ring (C-N=C) of heterocyclic compounds (Fig. 6c-d). Subsequently, the O 1s XPS continuum for CN and CN/BI<sub>10.0</sub> is depicted in Fig. S2.

The electronic paramagnetic resonance (EPR) results of CN and CN/BI<sub>10.0</sub> demonstrate a singular symmetric line with a g-value of 2.0034 at 3514 G (Fig. 7a). Under photoexcitation, the EPR conventions for CN/BI<sub>10.0</sub> are improving far faster than CN. The theory

behind this modification is the formation of large amounts of photocatalytic clusters within the framework of as-synthesized catalysts [52]. Similarly, the elemental composition was measured to quantify the number of each component within each sample (Fig. 7b). Because of molecular engineering, the outstanding sample CN/BI<sub>10.0</sub> exhibits a substantial percentage of constituents as well as a monetary quality of C/N ratio. The C/N molar ratios for all synthesized samples are displayed in Table. S1.

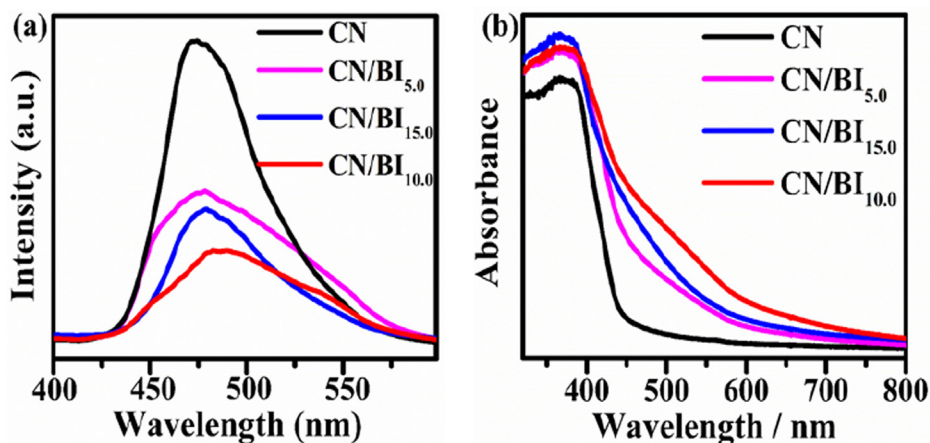


Fig. 4. (a) The optoelectronic absorbance wavelength and (b) photoluminescence spectral response of CN and CN/BI<sub>x</sub> materials under 400 nm excitation.

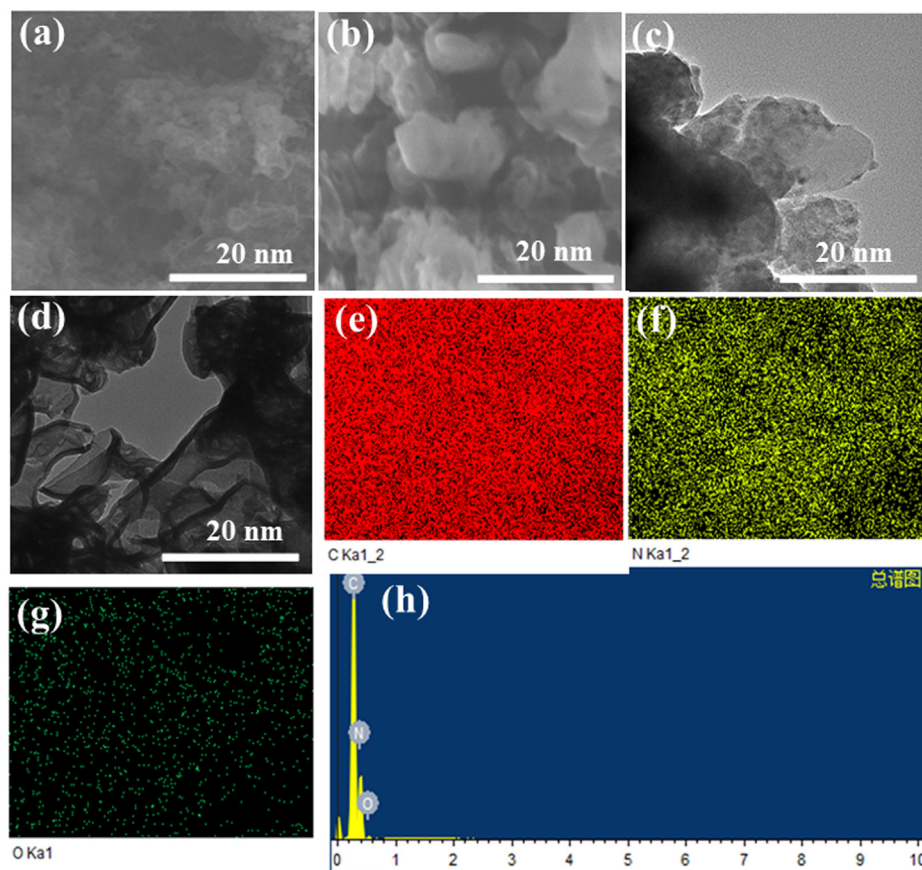


Fig. 5. (a, b) SEM illustrations of CN and CN/BI<sub>10.0</sub>, (c, d) TEM morphology of CN and CN/BI<sub>10.0</sub> and (e) is the elemental mapping of CN/BI<sub>10.0</sub> sample.

### 2.1. Density functional theory (DFT) and time-dependent DFT (TD-DFT).

The comprehensive reactant steps used for the fabrication of BI within the structure of CN are depicted in Fig. 1. The distribution of electronic energy was investigated using Gaussian 09 density functional theory (DFT) and time-dependent DFT (TD-DFT) methods for VB and CB configuration enhancement at the stage of B3LYP (beck three-parameter hybrid functional) /6-31G (d, p) [66]. It has been well demonstrated, that the numerous electron donor and acceptor components existing in an organic molecule exhibit particular

electronic structure due to the significant charge transmission (CT) function of their minimum excitons, allowing for comprehensive optical applications such as organic solar cells, organic transistors, etc. The highest occupied molecular orbital (HOMO) is mainly dispersed in D unit, and the lowest unoccupied molecular orbital (LUMO) is divided up in A unit. The existence of electron donor (D) and acceptor (A) substituents results in various gradients of specific isolation of the frontier molecular orbitals (FMOs). Reduced FMO intersect results in small energy splitting (EST) among the lowest singlet (S1) and triplet (T1) asserts. At ambient temperature, efficient up-conversion from T1 to S1 is possible,

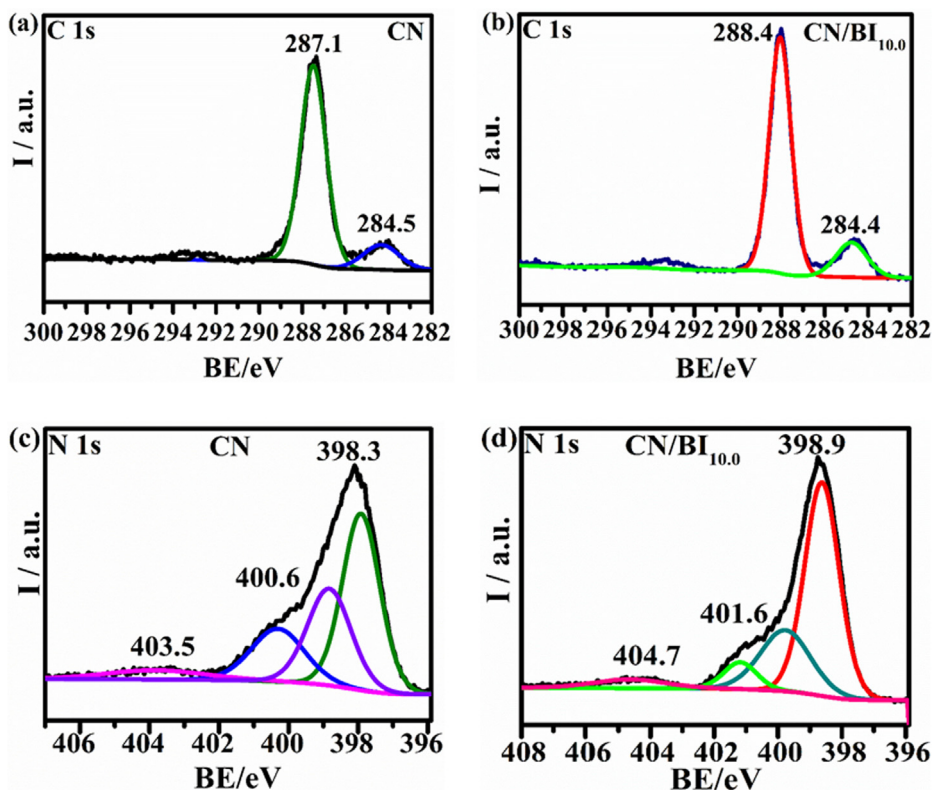


Fig. 6. (a) The XPS C 1s (a-b) and N 1s (c-d) spectrum for CN and CN/Bi<sub>10.0</sub> samples.

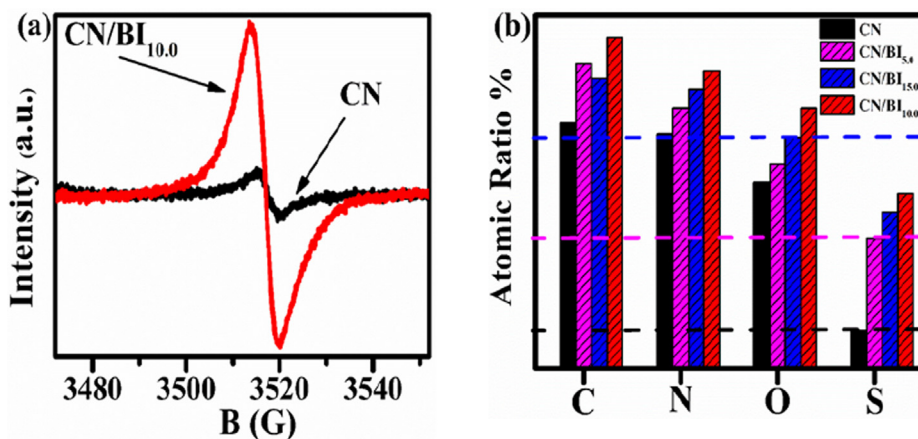


Fig. 7. (a) EPR spectra of CN and CN/Bi<sub>10.0</sub> (b) elemental assessment and C/N mass ratio for synthesized materials under visible light ( $\lambda > 420$  nm).

whenever the EST is limited sufficiently [66]. The energy band gap for CN, CN/Bi<sub>10.0</sub>, and CN/Bi<sub>15.0</sub> was observed as 4.375 eV, 3.731 eV, and 3.146 eV, as evaluated from the HOMO (-6.316 eV, -5.981 eV, and -6.581 eV) and LUMO (-1.897, -2.657 eV, and -2.152 eV) energy status. The energy states technique noted for CN, CN/Bi<sub>10.0</sub>, and CN/Bi<sub>15.0</sub> as well as the efficient intersystem crossing channels (ISC) implicated between lowest singlet (S1) and triplet (Tn) states have been calculated, as seen in Fig. 8.

### 3. Photocatalytic CO<sub>2</sub> Reduction Reaction

In the process, the materials were used for a photocatalytic CO<sub>2</sub> reduction reaction under visible light irradiation ( $\lambda > 420$  nm), which actually converts the CO<sub>2</sub> into CO and H<sub>2</sub> products. The pro-

cess reaction was carried out in aqueous media by containing acetonitrile (MeCN) and water addendum at 30 °C and 1 atm CO<sub>2</sub> with Co(bpy)<sub>3</sub><sup>2+</sup> as sensitizer and co-catalyst, and triethanolamine (TEOA) as a sacrificial electron donating entity (Comprehensive details in Supporting Information 2.5). Initially, constrained analyses were deducted, which affirmed that both light illumination and photocatalyst were required for CO<sub>2</sub> photocatalytic reaction. Furthermore, when purified Ar replaced CO<sub>2</sub> in the batch reactor, only H<sub>2</sub> was determined, thereby, indicating that the constituted carbon-containing products emerged from CO<sub>2</sub> but not contamination (Table. S2). The CO and H<sub>2</sub> were recognized as the primary CO<sub>2</sub> reduction products, and the assessment rates are shown in Fig. 9a. The products were detected employing gas chromatograph installed with a thermoelectric detection system which detected the CO. The dominant responses implicated in the photocatalytic

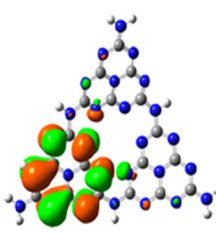
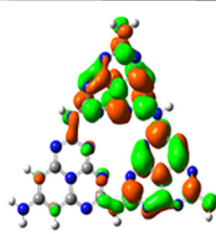
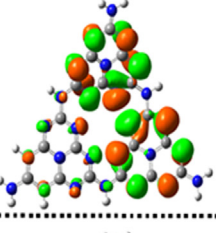
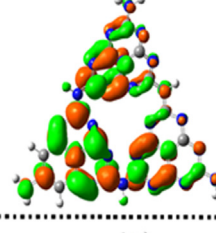
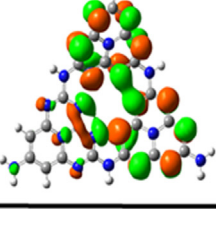
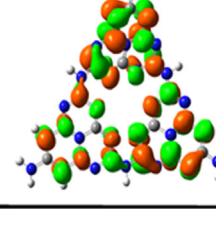
	Trimer 1		Trimer 2		$\Delta E_g$ (eV)
<u>CN/BI<sub>10.0</sub></u>					
Homo (-5.981eV)		LUMO -2.657eV			3.146
<u>CN/BI<sub>15.0</sub></u>					
Homo-1 (-6.581eV)		LUMO +1 -2.152eV			3.731
<u>CN</u>					
Homo-2 (-6.316eV)		LUMO +2 -1.897eV			4.375

Fig. 8. Electron charges distribution over HOMO and LUMO for as-prepared samples.

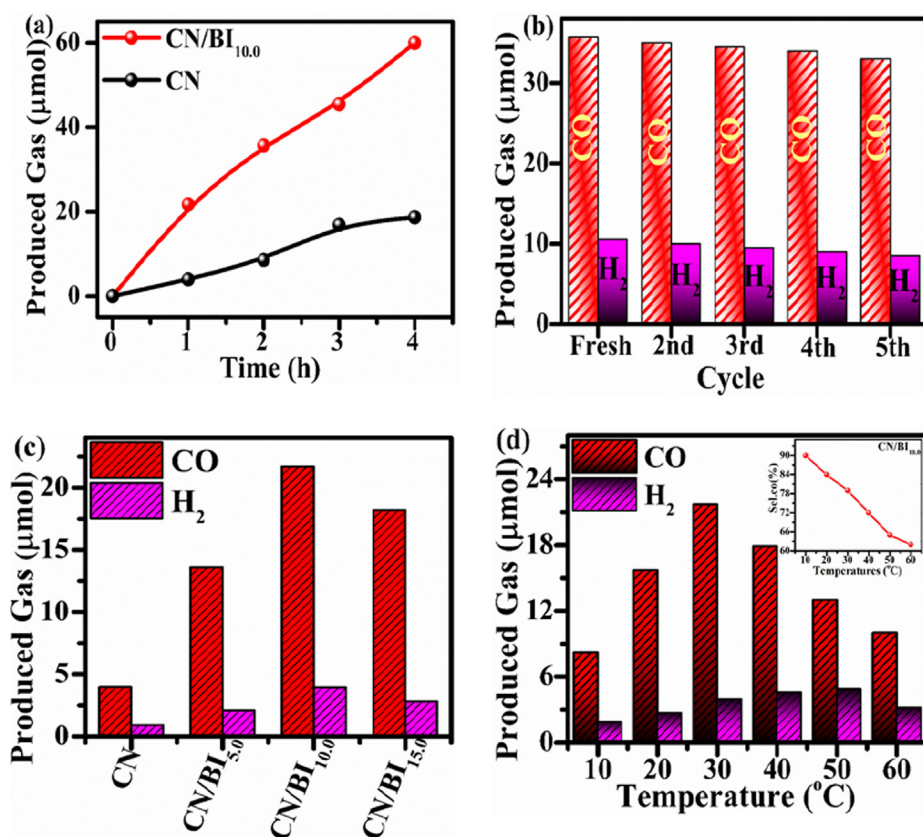
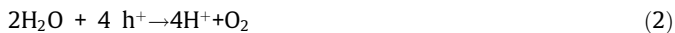


Fig. 9. Photocatalytic CO<sub>2</sub> reduction (a), Time function (b) persistent test for CN/BI<sub>10.0</sub> (c) different catalyst-based CO and H<sub>2</sub> production, (d) the CO<sub>2</sub> reduction under different temperature (Inset, selectivity of CN/BI<sub>10.0</sub>).

reduction of CO<sub>2</sub> with H<sub>2</sub>O in order to generate CO under visible light are summarized as follows.



According to the above integrals, the produced electrons (e<sup>-</sup>) and holes (h<sup>+</sup>) via light irradiation are important attributes for such photocatalytic process. Briefly, the electrons are energized from the VB to the CB and interact with the CO<sub>2</sub> molecule to produce CO, while the hole on the VB can oxidize H<sub>2</sub>O to produce oxygen (O<sub>2</sub>). As a result, the improved photocatalytic behavior of BI embedded CN catalysts may be due to the reduction replication of photoinduced electrons/holes pairs. As a result, after 4 h of visible irradiation, the reaction system generates 62.8 mol of CO and 18.1 mol of H<sub>2</sub>, thereby, emphasizing the maximum photocatalytic performance with regard to CO<sub>2</sub><sup>+</sup> (Fig. 9a). It was discovered that the existing system yields elevated precision of CO with a high output in the preliminary hours with regard to H<sub>2</sub>. Similarly, when the reaction time increased, the output steadily reduces due to the decomposition of the [Ru(bpy)<sub>3</sub>]Cl<sub>2</sub> sensitizers [67,68]. Furthermore, the photocatalytic efficiency of CO<sub>2</sub> reduction was drastically enhanced upon fluctuating the quantity of boozed BI in CN. Besides, protracted stability analyses were conducted in order to determine the consistency attribute of CN/BI<sub>10.0</sub> for the progression of CO and H<sub>2</sub> under visible light, as manifested in Fig. 9b. As a result, the outstanding catalyst display a small reduction in CO evolvment after each phase, thereby, implying its consistency as a catalyst for the median progress of CO with the proportion of cobalt species for every phase. Besides, accelerating the quantity of BI results in a decrease in photocatalytic performance, but greater than CN, which is dependent on the light absorption possessions generated by molecular engineering. Actually, the over-

abundance of monomer BI instantaneously destructs the conjugated configuration of CN, which results in a decrease of photocatalytic activity (Fig. 9c). The reaction process was investigated to determine the influence of accurate temperature zone on the evolvment of CO from CO<sub>2</sub> photoreduction, and thus the reaction system was inspected under varying temperature ranges (10–60 °C), as seen in Fig. 9d. The outcomes demonstrably show that the rate of CO multiplies as the temperature rises from 20 to 30 °C, and the CO<sub>2</sub> efficiency reaches a maximum of 25.2 mol/h<sup>1</sup> with a CO selectivity of 81.7 % for the reaction system (inset Fig. 9d). The results deduct the final conclusion, that the integration of BI within CN in turn improved the optical absorption circumstances and optimize the photoexcitation process are significant considerations in charge isolation and utilization in order to optimize photocatalytic performance.

#### 4. Photocatalytic H<sub>2</sub> Evolution

The H<sub>2</sub> evolution rate (HER) of CN catalyst is 58.4 mol/h, while that of modified CN/BI<sub>10.0</sub> catalyst exhibits a spectacular activity of 805.2 mol/h, that is approximately ten times higher than CN, as can be seen in Fig. 10a. Consequently, the outstanding CN/BI<sub>10.0</sub> photocatalyst were used for protracted recyclability and consistency analyses. The reaction system was run for five cycles (25 h), and no substantial alternation was observed, as exhibited in Fig. 10b. A minor decrease in behavior occurs after the third attempt due to a loosening interaction relationship between co-catalyst and photocatalyst. The consistency assessment reveals that CN/BI<sub>10.0</sub> displays amplified HER and excellent durability under visible irradiation. We conducted HER analyses under the same circumstances by contrasting various precursors of CN with their modified samples (Fig. 10c). Among these precursors, the total amount of BI monomer was established at 10.0 mg, that is correlated with the highest HER for CN/BI<sub>10.0</sub>. In comparison to other precursors, the analysis shows that urea comprising CN and their

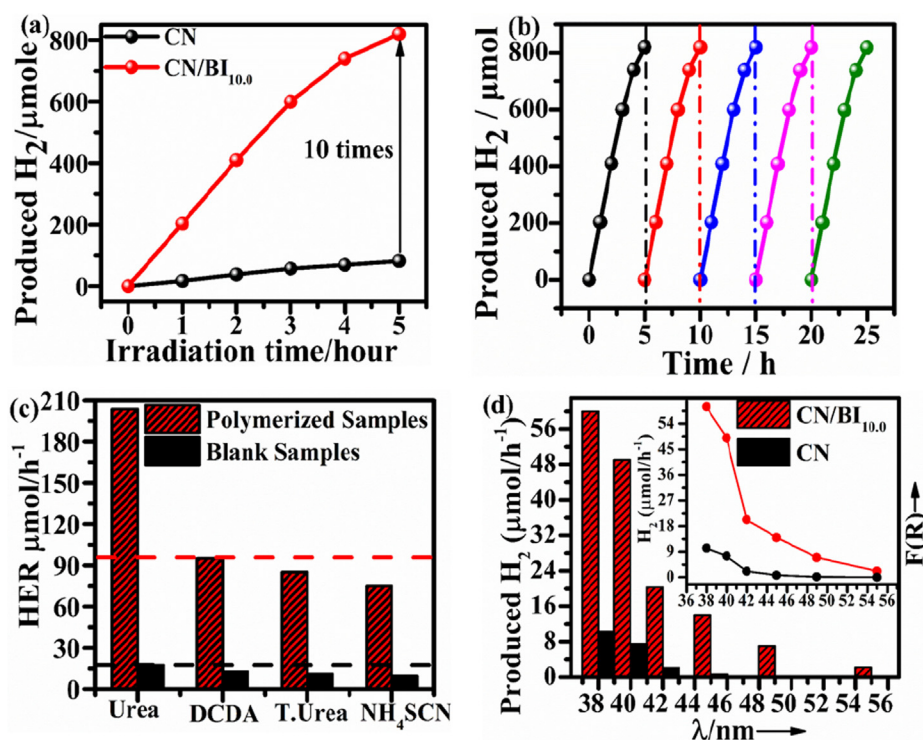
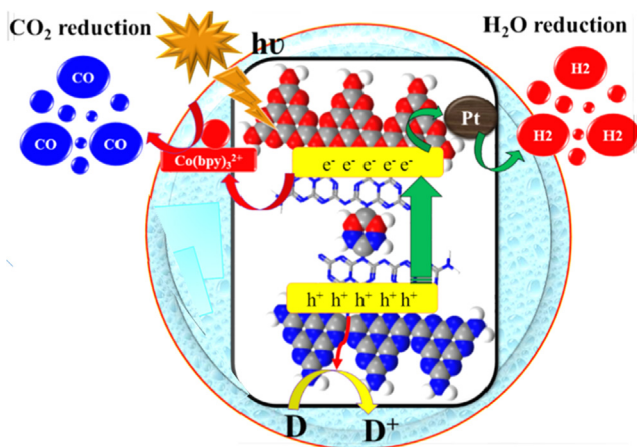


Fig. 10. Photocatalytic H<sub>2</sub> production (a) Time function (b) persistence analysis of CN/BI<sub>10.0</sub> Sample. (c) H<sub>2</sub> production over Urea (CN), DCDA, T. Urea (TCN), NH<sub>4</sub>SCN (ACN) and their modified catalysts. (d) Different wavelength HER b/w CN and CN/BI<sub>10.0</sub>.



**Fig. 11.** Schematic Photocatalytic mechanism for CN/Bi<sub>10.0</sub> sample under the illumination.

modified CN/Bi is the ideal photocatalyst under visible illumination. Result also demonstrate that the current monomer BI are boosting the activity of each CN precursor toward the noteworthy point. Additionally, multiple wavelength observations illustrate that the photocatalytic performance of CN/Bi<sub>10.0</sub> over CN enhanced all over the enormous visible spectral region (Fig. 10d). In comparison to CN/Bi<sub>10.0</sub>, the HER for CN is almost finished when the optical range is prolonged to 550 nm. In advisement to absorption, the overall photocatalytic attributes of CN/Bi<sub>10.0</sub> exhibit a massive wavelength HER. The Fig. S3 depicts the photocatalytic of HER using the outstanding CN/Bi<sub>10.0</sub> sample with other sacrificial agents.

## 5. Photocatalytic mechanism

Based on the data proffered above, the plausible photocatalytic sequence mechanism for H<sub>2</sub> evolution via CN/Bi<sub>10.0</sub> sample was evaluated under visible light stimulation, as shown in Fig. 11. When exposed to solar radiation, the CN/Bi<sub>10.0</sub> infringes on photons, and these photoinduced photons from the CB of CN/Bi<sub>10.0</sub> are launched to the external surface of sample's, where they contribute with counter-catalyst Pt particles. The photons produce H<sub>2</sub>, while the holes oxidize the TEOA, thereby, preventing charge replication and promoting photocatalytic performance. Significantly, H<sup>+</sup> is produced when water splits on the substrate of the catalyst, capturing electrons through Pt co-catalyst and thus producing H<sub>2</sub> energy. The sacrificial agent TEOA reduces the produced hole in the VB in this typical process. A large number of photoinduced electrons and holes are consumed together to reconstitute, while only a small number of photoexcited electrons are motivated and energized to accelerate the photocatalytic progression of hydrogen energy. Correspondingly, the photo CO<sub>2</sub> reduction emerges in the CB of the catalyst. Light activation generates electrons (e<sup>-</sup>) and holes (h<sup>+</sup>), which are important factors of this photocatalytic reaction. Subsequently, electrons are energized from VB to CB and interact with CO<sub>2</sub> molecules to produce CO, while holes in VB can oxidize H<sub>2</sub>O to produce oxygen (O<sub>2</sub>).

## 6. Conclusion

The incorporation and synthesis of dibromobenzimidazole (BI) monomer within the structure of CN was done deliberately. The BI is a unique organic monomer that composed aromatic benzene and furan ring which enhances optical absorption, optimizes the electronic structural band, promotes charge transport, and sepa-

rates photoinduced electrons/holes within CN. Correspondingly, due to the detrimental electrostatic interaction of nitrogen atoms, this monomer is constituted of the  $\pi$ -deficient aromatic group and  $\pi$ -electrons that are uniformly distributed over the ring of CN. The photocatalytic efficiency of CO<sub>2</sub> reduction into CO and water reduction, such as H<sub>2</sub> generation from water splitting, is significantly improved by the customized CN/Bi<sub>10.0</sub>. In summary, universal copolymerization investigates an extraordinary transformation by using a modest, optimized quantity of monomer BI with CN for elevated photocatalytic efficiency achievement. This cost-effective and minute integrated monomer establish the way for the innovation of a newly adapted photocatalyst in order to enhance the photocatalytic activity of CN in the progression of CO<sub>2</sub> reduction and HER.

## CRediT authorship contribution statement

**Zeeshan Ajmal:** Conceptualization, Methodology, Data curation, Formal analysis, Investigation, Writing - original draft. **T.A. Taha:** Visualization, Investigation. **Mohammed A. Amin:** Data curation, Writing - original draft. **Arkom Palamanit:** Data curation, Writing - original draft. **W.I. Nawawi:** Conceptualization, Methodology, Software. **Abul Kalam:** Software, Validation. **Abdullah G. Al-Sehemi:** Software, Validation. **Hamed Algarni:** Software, Validation. **Abdul Qadeer:** Software, Validation. **Hamid Ali:** Software, Validation. **Anuj Kumar:** Data curation, Writing - original draft. **Jin Qian:** Funding acquisition, Writing - review & editing. **Asif Hayat:** Conceptualization, Methodology, Software, Formal analysis, Writing - original draft, Writing - review & editing. **Huaqiang Zeng:** Supervision, Conceptualization, Funding acquisition, Project administration, Writing - review & editing.

## Data availability

The data that has been used is confidential.

## Declaration of Competing Interest

There is no no known competing financial interests or personal relationships that could be appeared to influence the work reported in this paper.

## Acknowledgement

Authors acknowledge support and funding of King Khalid University through Research Center for Advanced Materials Science (RCAMS) under grant no: RCAMS/KKU/0010/21. The authors are also grateful to the Taif University Researchers Supporting Project number (TURSP-2020/03), Taif University, Taif, KSA.

## Appendix A. Supplementary data

Supplementary data to this article can be found online at <https://doi.org/10.1016/j.molliq.2022.120617>.

## References

- [1] F. Raziq, A. Hayat, M. Humayun, S. Mane, Q. Liang, *Appl. Catal. B* (2020).
- [2] S. Ghufuran, Z. Arif, Q.U. Hassan, M. Mohsin, A. Hayat, Second iScience International Conference 2021: Recent Advances in Photonics and Physical Sciences, 2021.
- [3] I. Ullah, T.A. Taha, A.M. Alenad, I. Uddin, A. Hayat, A. Hayat, M. Sohail, A. Irfan, J. Khan, A. Palamanit, *Surf. Interfaces* (2021).
- [4] A.U. Rehman, M. Khan, M. Zheng, A.R. Khan, A. Hayat, *Heat Mass Transf.* (2020).
- [5] I. Uddin, G. Wang, D. Gao, Z. Hussain, A. Hayat, *Biomass Conversion and Biorefinery* (2021).
- [6] F. Raziq, J. He, J. Gan, M. Humayun, L. Qiao, *Appl. Catal. B* 270 (2020).



- [7] Z. Ajmal, M. Usman, I. Anastopoulos, A. Qadeer, R. Zhu, A. Wakeel, R. Dong, J. Environ. Manage. 264 (2020).
- [8] A. Hayat, F. Raziq, M. Khan, I. Ullah, M. Ur Rahman, W.U. Khan, J. Khan, A. Ahmad, J. Photochem. Photobiol., A 379 (2019) 88.
- [9] A. Hayat, N. Shaishta, S.K.B. Mane, J. Khan, A. Hayat, A.C.S. Appl. Mater. Interfaces 11 (2019) 46756.
- [10] S. Ahmed, H.U. Rehman, Z. Ali, A. Qadeer, A. Haseeb, Z. Ajmal, Surf. Interf. 23 (2021).
- [11] A. Hayat, A.G. Al-Sehemi, K.S. El-Nasser, T.A. Taha, A.A. Al-Ghamdi, S. Jawad Ali Shah, M.A. Amin, T. Ali, T. Bashir, A. Palamanit, J. Khan, W.I. Nawawi, Int. J. Hydrogen Energy 47 (2022) 5142.
- [12] A. Qadeer, K.L. Kirsten, Z. Ajmal, X. Jiang, X. Zhao, Environ. Sci. Technol. 56 (2022) 1482.
- [13] A. Qadeer, K.L. Kirsten, Z. Ajmal, Z. Xingru, Environ. Sci. Technol. 56 (2022) 5294.
- [14] A. Qadeer, Z.A. Saqib, Z. Ajmal, C. Xing, S. Khan Khalil, M. Usman, Y. Huang, S. Bashir, Z. Ahmad, S. Ahmed, K.H. Thebo, M. Liu, Sustain. Cities. Soc. 53 (2020) 101959.
- [15] A.M. Appel, J.E. Bercaw, A.B. Bocarsly, H. Dobbek, D.L. DuBois, M. Dupuis, J.G. Ferry, E. Fujita, R. Hille, P.J. Kenis, Chem. Rev. 113 (2013) 6621.
- [16] F. Sastre, A. Corma, H. Garcia, J. Am. Chem. Soc. 134 (2012) 14137.
- [17] L. Liu, H. Zhao, J.M. Andino, Y. Li, ACS Catal. 2 (2012) 1817.
- [18] W. Fan, Q. Zhang, Y. Wang, PCCP 15 (2013) 2632.
- [19] H. Yin, Z. Tang, ChemCatChem 7 (2015) 904.
- [20] R. Kuriki, K. Sekizawa, O. Ishitani, K. Maeda, Angew. Chem. Int. Ed. 54 (2015) 2406.
- [21] Z. Ajmal, A. Muhmood, R. Dong, S. Wu, J. Environ. Manage. 253 (2020).
- [22] H. Ali, S. Ahmed, A. Hsini, S. Kizito, Y. Naciri, R. Djellabi, M. Abid, W. Raza, N. Hassan, M.S. Rehman, A. Jamal Khan, M. Khan, M. Zia Ul Haq, D. Aboagye, M.K. Irshad, M. Hassan, A. Hayat, B. Wu, A. Qadeer, Z. Ajmal, Arab. J. Chem. (2022) 104209.
- [23] A. Ah, B. Ns, C. lu, D. Mk, E. Skbmb, F. Ah, G. lu, H. Aur, I. Ta, J. Gm, J. Colloid Interface Sci. (2021).
- [24] N. Arif, I. Uddin, A. Hayat, W.U. Khan, S. Ullah, M. Hussain, Polymer International (2021).
- [25] Z. Ajmal, A. Muhmood, M. Usman, S. Kizito, J. Lu, R. Dong, S. Wu, J. Colloid. Interf. Sci 528 (2018) 145.
- [26] Z. Ajmal, Y. Naciri, A. Hsini, B.M. Bresolin, A. Qadeer, M. Nauman, M. Arif, M.K. Irshad, K.A. Khan, R. Djellabi, C.L. Bianchi, M. Laabd, A. Albourine, R. Dong, in: N.A. Oladoja, E.I. Unuabonah (Eds.), Progress and Prospects in the Management of Oxyanion Polluted Aqua Systems, Springer International Publishing, Cham, 2021, pp. 185–217.
- [27] W. Li, M. Sohail, U. Anwar, T.A. Taha, A.G. Al-Sehemi, S. Muhammad, A.A. Al-Ghamdi, M.A. Amin, A. Palamanit, S. Ullah, A. Hayat, Z. Ajmal, Int. J. Hydrogen Energy 47 (2022) 21067.
- [28] J.M. McEnaney, J.C. Crompton, J.F. Callejas, E.J. Popczun, A.J. Biacchi, N.S. Lewis, R.E. Schaak, Chem. Mater. 26 (2014) 4826.
- [29] T.A. Taha, M.H. Mahmoud, A. Hayat, A. Irfan, (2021).
- [30] Z. Ajmal, M.u. Haq, Y. Naciri, R. Djellabi, N. Hassan, S. Zaman, A. Murtaza, A. Kumar, A.G. Al-Sehemi, H. Algarni, O.A. Al-Hartomy, R. Dong, A. Hayat, A. Qadeer, Chemosphere 308 (2022) 136358.
- [31] F. Ali, M. Sohail, T.A. Taha, A.G. Al-Sehemi, S. Ullah, H.S. AlSalem, G.A.M. Mersal, M.M. Ibrahim, A.M. Alenad, O.A. Al-Hartomy, M.A. Amin, Z. Ajmal, A. Palamanit, A. Hayat, A. Zada, W.I. Nawawi, Mater. Res. Bull. 152 (2022).
- [32] H. Asif, S. Naghma, K. Sunil, M. Baburao, K. Javid, ACS Appl. Mater. Interfaces 11 (2019) 46756.
- [33] A. Ah, B. Ns, C. Skbm, D. Ah, E. Jk, F. Aur, G. Ti, J. Colloid Interface Sci. 560 (2020) 743.
- [34] A. Hayat, F. Raziq, M. Khan, J. Khan, W.U. Khan, J. Colloid Interface Sci. 554 (2019).
- [35] M.U. Rahman, A. Hayat, Int. J. Energy Res. (2019).
- [36] C. Gao, Q. Meng, K. Zhao, H. Yin, D. Wang, J. Guo, S. Zhao, L. Chang, M. He, Q. Li, Adv. Mater. 28 (2016) 6485.
- [37] A.J. Bard, M.A. Fox, Acc. Chem. Res. 28 (1995) 141.
- [38] K. Maeda, K. Teramura, D. Lu, T. Takata, N. Saito, Y. Inoue, K. Domen, Nature 440 (2006) 295.
- [39] A. Hayat, T. Li, Int. J. Energy Res. 43 (2019).
- [40] A. Hayat, F. Raziq, M. Khan, I. Ullah, W.U. Khan, J. Photochem. Photobiol., A (2019).
- [41] A. Hayat, M. Sohail, A. Qadeer, T.A. Taha, M. Hussain, S. Ullah, A.G. Al-Sehemi, H. Algarni, M.A. Amin, M. Aqeel Sarwar, W.I. Nawawi, A. Palamanit, Y. Orooji, Z. Ajmal, Chem. Rec. n/a (2022) e202200097.
- [42] L. Lin, H. Ou, Y. Zhang, X. Wang, ACS Catal. 6 (2016) 3921.
- [43] A. Hamid, M. Khan, A. Hayat, J. Raza, F. Hussain, Spectrochimica Acta Part A Molecular and Biomolecular, Spectroscopy 235 (2020).
- [44] A. Hayat, M.U. Rahman, I. Khan, J. Khan, M. Sohail, H. Yasmeen, S.Y. Liu, K. Qi, W. Lv, Molecules 24 (2019).
- [45] A. Hayat, M. Sohail, U. Anwar, T.A. Taha, K.S. El-Nasser, A.M. Alenad, A.G. Al-Sehemi, N. Ahmad Alghamdi, O.A. Al-Hartomy, M.A. Amin, A. Alhadhrami, A. Palamanit, S.K.B. Mane, W.I. Nawawi, Z. Ajmal, J. Colloid Interface Sci. 624 (2022) 411.
- [46] A. Hayat, M. Sohail, T.A. Taha, S. Kumar Baburao Mane, A.G. Al-Sehemi, A.A. Al-Ghamdi, W.I. Nawawi, A. Palamanit, M.A. Amin, A.M. Fallatah, Z. Ajmal, H. Ali, W. Ullah Khan, M. Wajid Shah, J. Khan, S. Wageh, J. Colloid Interface Sci. 627 (2022) 621.
- [47] M. Sohail, U. Anwar, T.A. Taha, H.I.A. Qazi, A.G. Al-Sehemi, S. Ullah, H. Algarni, I. M. Ahmed, M.A. Amin, A. Palamanit, W. Iqbal, S. Alharthi, W.I. Nawawi, Z. Ajmal, H. Ali, A. Hayat, Arab. J. Chem. 15 (2022).
- [48] G. Zhang, J. Zhang, M. Zhang, X. Wang, J. Mater. Chem. 22 (2012) 8083.
- [49] Y. Cui, J. Zhang, G. Zhang, J. Huang, P. Liu, M. Antonietti, X. Wang, J. Mater. Chem. 21 (2011) 13032.
- [50] J. Zhang, J. Sun, K. Maeda, K. Domen, P. Liu, M. Antonietti, X. Fu, X. Wang, Energy Environ. Sci. 4 (2011) 675.
- [51] J. Liu, Y. Zhang, L. Lu, G. Wu, W. Chen, Chem. Commun. 48 (2012) 8826.
- [52] G. Dong, L. Zhang, J. Mater. Chem. 22 (2012) 1160.
- [53] X. Wang, S. Blechert, M. Antonietti, ACS Catal. 2 (2012) 1596.
- [54] A. Hayat, J.K. han, M.U. Rahman, S.B. Mane, W.U. Khan, M. Sohail, N.U. Rahman, N. Shaishta, Z. Chi, M. Wu, J. Colloid Interface Sci. (2019).
- [55] A. Hayat, J.A. Shah Syed, A.G. Al-Sehemi, K.S. El-Nasser, T.A. Taha, A.A. Al-Ghamdi, M.A. Amin, Z. Ajmal, W. Iqbal, A. Palamanit, D.I. Medina, W.I. Nawawi, M. Sohail, Int. J. Hydrogen Energy 47 (2022) 10837.
- [56] W. Che, W. Cheng, T. Yao, F. Tang, W. Liu, H. Su, Y. Huang, Q. Liu, J. Liu, F. Hu, J. Am. Chem. Soc. 139 (2017) 3021.
- [57] A. Hayat, M. Sohail, T.A. Taha, A.M. Alenad, S. Mane, Catalysts 11 (2021).
- [58] A. Hayat, Z.A. Alrowaili, T.A. Taha, J. Khan, W.U. Khan, Synth. Met. (2021).
- [59] A. Hayat, M. Sohail, W. Iqbal, T.A. Taha, A.M. Alenad, A.G. Al-Sehemi, S. Ullah, N. A. Alghamdi, A. Alhadhrami, Z. Ajmal, A. Palamanit, W.I. Nawawi, H.S. AlSalem, H. Ali, A. Zada, M.A. Amin, J. Sci.: Adv. Mater. Devices (2022).
- [60] J. Zhang, X. Chen, K. Takanabe, K. Maeda, K. Domen, J.D. Epping, X. Fu, M. Antonietti, X. Wang, Angew. Chem. Int. Ed. 49 (2010) 441.
- [61] A. Hayat, T.A. Taha, A.M. Alenad, I. Ullah, S. Shah, I. Uddin, I. Ullah, A. Hayat, W. U. Khan, Surf. Interfaces (2021).
- [62] A. Ullah, J. Khan, M. Sohail, A. Hayat, W.U. Khan, J. Photochem. Photobiol., A 401 (2020).
- [63] D.F. Raizq, J. Electrochem. Soc. (2020).
- [64] Z. Maosheng, A.U. Rehman, A. Hayat, Int. J. Energy Res. (2020).
- [65] N. Shaishta, W.U. Khan, S.K.B. Mane, A. Hayat, G. Manjunatha, Int. J. Energy Res. (2020).
- [66] T. Toivonen, T.I. Hukka, J. Phys. Chem. A 111 (2007) 4821.
- [67] Z. Ding, X. Chen, M. Antonietti, X. Wang, ChemSusChem 4 (2011) 274.
- [68] A. Dhakshinamoorthy, S. Navalon, A. Corma, H. Garcia, Energy Environ. Sci. 5 (2012) 9217.